

# Investigation of trapping/detrapping mechanisms in Al<sub>2</sub>O<sub>3</sub> electron/hole traps and their influence on TANOS memory operations

Luca Larcher<sup>1</sup>, Andrea Padovani<sup>1</sup>, Vincenzo della Marca<sup>2</sup>, Paolo Pavan<sup>2</sup>, Alessandro Bertacchini<sup>1</sup>

<sup>1</sup>DISMI, Università di Modena e Reggio Emilia, and IU.NET, Via Amendola 2, 42122 Reggio Emilia, Italy

<sup>2</sup>DII, Università di Modena e Reggio Emilia, and IU.NET, Via Vignolese 905, 41100 Modena, Italy

[luca.larcher@unimore.it](mailto:luca.larcher@unimore.it)

Alumina is a key material for developing innovative Charge-Trapping Non-Volatile Memory (CT-NVM) devices. Al<sub>2</sub>O<sub>3</sub> is used to implement the top dielectric in TANOS devices [1], and it has been proposed as trapping layer [2] and to engineer the tunnel dielectric [3]. Despite the large use of this material, the quantitative investigation of defect features still lacks. *In this scenario, the purpose of this work is to investigate the physics of electron/hole trapping/detrapping mechanisms in Al<sub>2</sub>O<sub>3</sub>. Combining I-V and C-V measurements with a physical model we derive the energy levels of electron/hole traps and the location of electron/hole charge. The influence of electron/hole alumina traps on TANOS operations and reliability is investigated.*

We developed a combined I-V and C-V measurement scheme: 1) C-V on fresh device; 2) I-V measure performed applying a gate voltage  $V_G$  ramp (0.1V/s) from 0 to  $V_{G,MAX}$ ; 3) C-V; 4) I-V varying  $V_G$  from  $V_{G,MAX}$  to  $V_{G,MIN}$ ; 5) C-V; 6) I-V varying  $V_G$  from  $V_{G,MIN}$  to 0.  $V_{G,MAX}$  and  $V_{G,MIN}$  are selected to limit the maximum current density to  $\sim 100$  mA/cm<sup>2</sup> in order to prevent the dielectric breakdown. Devices used are large area ( $\sim 9.18E-3$  cm<sup>2</sup>) n-MOS capacitors with TiN/Al<sub>2</sub>O<sub>3</sub>/SiO<sub>2</sub>/Si stack, manufactured using standard process. Alumina thicknesses are  $t_{Al}=5, 10$  and  $15$ nm, with a thin ( $\sim 1$  nm) interfacial SiO<sub>x</sub> layer at the Si interface. Thicknesses and relative dielectric constants of interfacial SiO<sub>x</sub> ( $k_{SiOx}=5$  [5]) and Al<sub>2</sub>O<sub>3</sub> ( $k_{Al2O3}=9.15$ ) layers are extracted from C-V measurements. Fig. 1 shows C-V curves measured on samples with  $t_{Al}=15$ nm. Simulations performed using the model in [6] reproduce accurately the measurements. For virgin devices, we assumed a fixed electron charge density  $\sim 10^{12}$  e/cm<sup>2</sup> at the SiO<sub>x</sub>/Al<sub>2</sub>O<sub>3</sub> interface, attributed to the process. Fig. 2 shows I-V curves measured on the  $t_{Al}=15$ nm capacitor. I-V characteristics show a significant hysteresis especially at positive  $V_G$ , indicating that electron trapping occurs during the  $V_G=0-16$ V ramp. This is confirmed also by the C-V curve measured after the  $V_G=0-16$ V ramp, showing a positive shift of the flat-band voltage  $\Delta V_{FB}=1.6$ V. Negligible hysteresis is observed at negative  $V_G$ , whereas C-V curves measured after the negative  $V_G$  ramp shows a significant  $\Delta V_{FB}=-1.6$ V, indicating a large hole trapping in the SiO<sub>x</sub>/Al<sub>2</sub>O<sub>3</sub> stack. Despite the same  $|\Delta V_{FB}|$  after positive and negative  $V_G$  ramps, the larger I-V curve hysteresis observed with  $V_G > 0$  indicates that electron traps are much slower than hole ones. This result is not affected by the relative sequence of positive and negative I-V. We repeated the same experiment on devices with  $t_{Al}=10$  nm. Again, we found that I-V hysteresis is significant especially for positive  $V_G$ . C-V curves measured after negative  $V_G$  ramp shows a negative  $\Delta V_{FB}=-0.76$ V, confirming that hole trapping is significant. We investigated also samples with  $t_{Al}=5$ nm, observing neither I-V hysteresis nor flat band voltage shift after both positive and negative  $V_G$  ramp. This indicates that electron and hole trapping is negligible for  $t_{Al}$  thinner than 5 nm.  $V_{FB}$  shifts after positive and negative  $V_G$  ramps are plotted versus  $t_{Al}$  in the inset of Fig. 1. The  $\Delta V_{FB}$  reduction with decreasing  $t_{Al}$  is due to the lower electron/hole charge trapped within the Al<sub>2</sub>O<sub>3</sub> stack. Since  $\Delta V_{FB}$  is negligible for the  $t_{Al}=5$ nm capacitors, we conclude that the charge trapping at the SiO<sub>x</sub>/Al<sub>2</sub>O<sub>3</sub> interface is not dominant. The charge is thus expected to be distributed across the Al<sub>2</sub>O<sub>3</sub> volume.

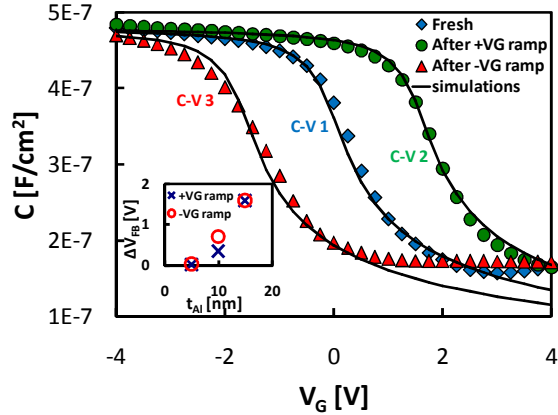


FIGURE 1. C-V CURVES SIMULATED (SOLID LINES) AND MEASURED ON FRESH DEVICE (CIRCLES), AFTER VG RAMP FROM 0V TO  $V_{G,MAX}$  (TRIANGLES), AFTER VG RAMP FROM  $V_{G,MAX}$  TO  $V_{G,MIN}$  (SQUARE). THE INSET SHOWS THE  $\Delta V_{FB}$  MEASURED AFTER POSITIVE AND NEGATIVE VG RAMP FOR DIFFERENT ALUMINA THICKNESSES.

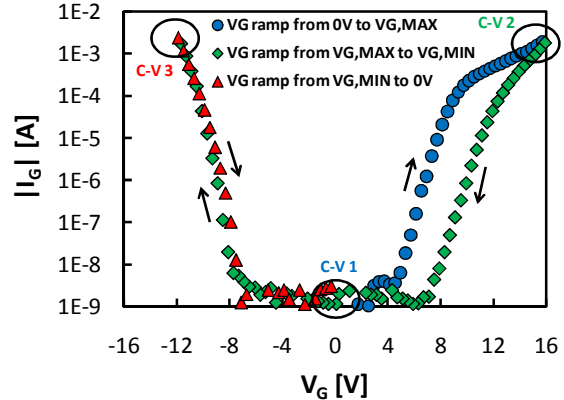


FIGURE 2. I-V CURVES MEASURED ON  $t_{Al}=15$ NM CAPACITORS.

To derive the energy distribution of electron/hole traps we performed retention experiments after positive and negative  $V_G$  ramps.  $\Delta V_{FB}$  curves measured during retention experiments at different temperatures are shown in Fig. 3. The temperature does not affect  $\Delta V_{FB}$  in retention, see empty symbols, suggesting that charge detrapping is mainly due to tunneling emission rather than thermally activated mechanisms. We use the model in [7] to reproduce the experimental data and to calculate the energy levels for defects. The time evolution of the trapped electron/hole charge is determined by solving self-consistently current continuity and Poisson equations including drift and diffusion mechanisms. Tunneling currents through bottom oxide and alumina blocking layers include direct/FN/modified tunneling contributions, Trap-to-Band Tunneling (TBT) and Trap-Assisted-Tunneling (TAT). Trapping is described according the SRH theory, while detrapping accounts for thermal emission (TE) and TBT contributions.  $\Delta V_{FB}$  simulations in Fig. 3 performed considering unbiased samples agree very accurately with measurements. Noticeably, a unique set of trap parameters is

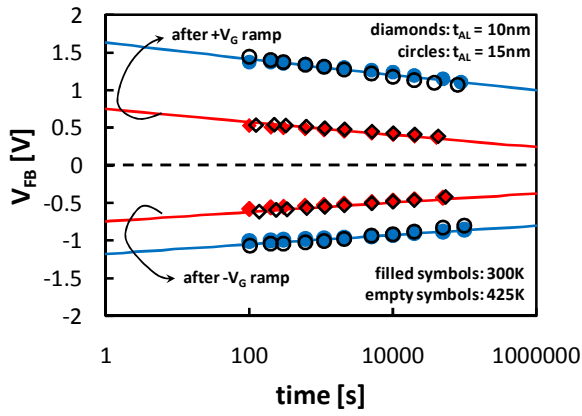


FIGURE 3. IV CURVES MEASURED (SYMBOLS) AND SIMULATED (SOLID LINES) USING THE MODEL IN [2] ON DEVICES WITH  $t_{AL}=15\text{NM}$  AND  $t_{AL}=10\text{NM}$  AFTER POSITIVE ( $\Delta V_{FB}>0$ ) AND NEGATIVE ( $\Delta V_{FB}<0$ )  $V_G$  RAMPS.

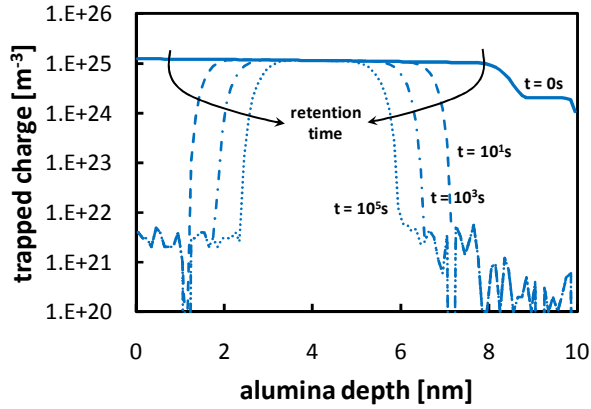


FIGURE 4. ELECTRON CHARGE EVOLUTION DERIVED FROM RETENTION SIMULATIONS ON DEVICES WITH 10 NM THICK ALUMINA.

considered independently of  $t_{AL}$ . The energy levels for electrons are deeper ( $E_T=2.0\text{-}2.6$  eV) than hole ones ( $E_T=1.6\text{-}2.2\text{eV}$ ), demonstrating that electron detrapping is slower due to the higher tunneling barrier of trapped electrons. Simulations allow deriving also the location of electron and hole charge inside the  $\text{Al}_2\text{O}_3$  and its evolution over time in retention, see Fig. 4. As expected, electrons trapped close to the  $\text{Al}_2\text{O}_3$  interfaces escape immediately, explaining the lower charge found in thinner  $\text{Al}_2\text{O}_3$  capacitors, i.e. trends of retention and I-V hysteresis measurements.

Charge trapping in  $\text{Al}_2\text{O}_3$  layer affects TANOS memory operation and reliability, contributing significantly to the  $V_{FB}$  shifts in both retention and P conditions. Using the model in [7], we reproduce accurately  $\Delta V_{FB}$  evolution during program in TANOS devices, see Fig. 5. The charge distribution calculated after program shows a significant electron trapping in the alumina, see Fig. 6. This is also confirmed by the  $V_{FB}$  shift observed in retention conditions, performed applying a large gate voltage  $V_G=6\text{V}$  to accelerate the charge loss, see Fig. 7. The  $\Delta V_{FB}$  curve shows a double slope over time well reproduced by simulations, related to the presence of electrons trapped in the alumina layer. Thanks to the much higher tunneling probability, electrons in alumina traps escape much faster compared to electrons in the nitride, determining the double-slope  $V_T$  curve. This behavior cannot be reproduced by simulations without considering electron trapping in  $\text{Al}_2\text{O}_3$ , see dashed line, and is more and more evident with increasing  $V_G$ . Simulations show that electron trapping in the alumina can contribute up to the 15% of the total  $V_{FB}$  shift.

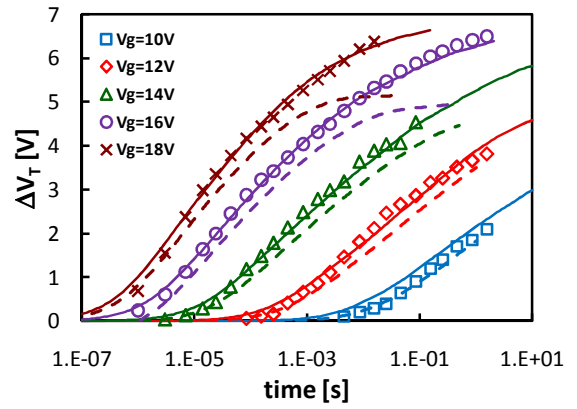


FIGURE 5. I-V CURVES MEASURED (SYMBOLS) ON TANOS CAPACITORS WITH 15NM/4NM/4.5NM ALUMINA/NITRIDE/OXIDE THICKNESSES. SIMULATIONS ARE PERFORMED TAKING INTO ACCOUNT (SOLID LINES) AND NEGLECTING (DASHED LINES) CHARGE TRAPPING INTO THE ALLUMINA LAYER.

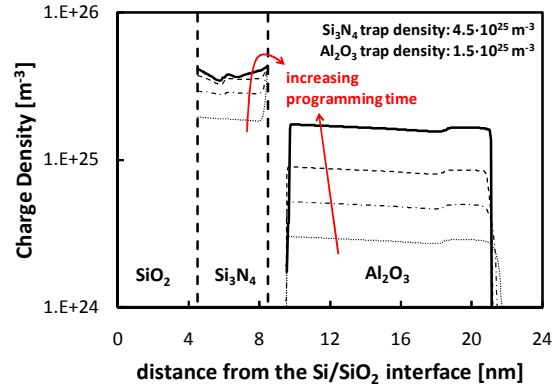


FIGURE 6. ELECTRON CHARGE DISTRIBUTION DERIVED FROM PROGRAM SIMULATIONS PERFORMED WITH THE MODEL IN [2] CONSIDERING A TANOS STACK WITH 4.5/4/15 NM OXIDE/NITRIDE/ALUMINA.

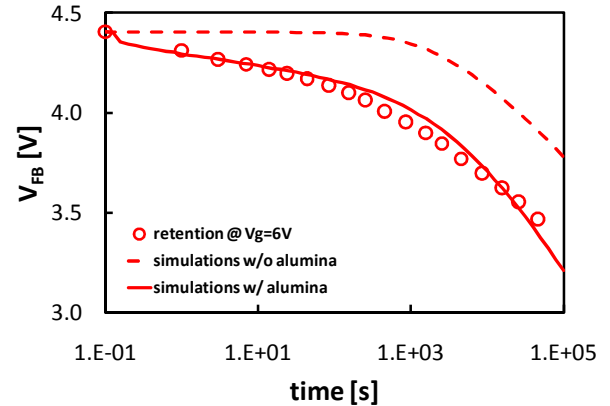


FIGURE 7.  $\Delta V_{FB}$  MEASURED (SYMBOLS) AND SIMULATED TAKING INTO ACCOUNT (SOLID LINES) AND NEGLECTING (DASHED LINES) ELECTRON TRAPPING IN THE ALLUMINA LAYER IN RETENTION CONDITIONS APPLYING  $V_G=6\text{V}$  TO ACCELERATE THE CHARGE LOSS.

## REFERENCES

- [1] Y. Park *et al.*, IEDM Tech. Dig., pp. 29-32, 2006.
- [2] J. Robertson, Rep. Prog. Phys. 69, pp. 327-396, 2006.
- [3] T. Sugizaki *et al.*, VLSI Tech. Digest, pp. 27-28, 2003.
- [4] P. Blomme *et al.*, International Memory Workshop, 2009.
- [5] F. Giustino *et al.*, vol. 72, pp. 299-303, 2004.
- [6] L. Larcher *et al.*, IEEE TED, Vol. 48(5), pp.935-945, 2001.
- [7] A. Padovani *et al.*, IEEE EDL, Vol. 30(8), pp. 882-884, 2009.